16th European Signal Processing Conference (EUSIPCO 2008), Lausanne, Switzerland, August 25-29, 2008, copyright by EURASIP

NOISE ESTIMATION OF POLARIZATION-ENCODED IMAGES BY PEANO-HILBERT FRACTAL PATH

Samia Ainouz[1], Jihad Zallat[2] and Fabrice Meriaudeau[1]

Laboratoire d'Electronique, Informatique et Image (LE2I), UMR CNRS 5158, Burgundy University
[1]LE2I, 12 rue de la fonderie, 71200, Le Creusot, France [2]LSIIT, Bd Sébastien Brant, 67400, Strasbourg, France
phone: + (33) 385731129, fax: + (33) 385731097, email: samia.ainouz@u-bourgogne.fr

ABSTRACT

In the framework of Stokes parameters imaging, polarization-encoded images have four channels. The potential of such multidimensional structure comes from the set of physical information they carry about the local nature of the target. However, the noise that affects the intensity measurement may induce the non physical meaning of Stokes parameters making awkward their analysis and interpretation. This induces the need for a proper tool that allows the processing of polarization-encoded images while respecting their physical content. In this paper a new method to filter the additive noise of polarimetric measurement is addressed. This method is based on two multispectral filtering methods combined with a transformation of Stokes channels following a fractal path. The proposed algorithm is a tradeoff between the filtering of polarization-encoded images and the preserving of their physical content. The statistical performances of the method are tested on simulated and real images using Bootstrap re-sampling.

1. INTRODUCTION

Polarization-sensitive imaging systems have emerged as a very attractive vision technique which can reveal important information about the physical and geometrical properties of the targets. Many imaging polarimeters have been designed in the past for several fields, ranging from metrology to medical and remote sensing applications [1], [2].

Imaging systems, that can measure the polarization state of the outgoing light across a scene, are mainly based on the ability to build effective Polarization State Analyzers (PSA) in front of the camera enabling to acquire the Stokes vectors [1]. These Stokes polarimeters produced four images called "Stokes images" corresponding to the four Stokes parameters. Accordingly, polarization-encoded images have a multidimensional structure; i.e. multi-component information is attached to each pixel in the image. Moreover, the information content of polarization-encoded images is intricately combined in the polarization channels making awkward their proper interpretation in the presence of noise.

Noise is inherent to any imaging systems and it is therefore present on Stokes images. It is of additive nature when the scene is illuminated by incoherent light and multiplicative when the illumination is coherent [3], [4]. Its presence degrades the interpretability of the data and prevents from exploring the physical potential of polarimetric information. Few works in the literature addressed the filtering of polarimetric images. We note nevertheless the use of optimization methods by [5] to optimize imaging system parameters that condition signal to noise ratio, or the improvement of the accuracy of the degree of polarization by [3] with the aim of reducing the noise in Stokes images.

The main problem in filtering polarization-encoded images is to respect their physical content. Therefore, a tradeoff has to be reached so as to minimize the effect of the noise affecting polarimetric images and to preserve their physical meaning.

In this paper, images being acquired under incoherent illumination, additive noise is estimated and eliminated such that the physical content of the polarimetric images is preserved as much as possible. The estimation methods are chosen in the range of multispectral filtering methods. In order to take advantage of both methods, the filtering algorithm deals with a combination of Scatter plot [6] and data masking methods [4]. As the information content of polarization-encoded images is intricately combined in several polarization channels, Peano-Hilbert fractal path is applied on the noisy image to keep the connexity of homogeneous areas and to minimize the impact of the outliers. The performances and the bias of the method are statistically investigated by Bootstrap method [7].

2. POLARIZATION IMAGE ACQUISITION

Acquisition of Stokes images is presented herein as well as the additive noise that affects polarization measurements.

2.1 Stokes imaging

The general polarization state of a light wave can be described by the so called Stokes vector S which fully characterizes the time-averaged polarization properties of a radiation. It is defined by the following combination of complex-valued components E_x and E_y of the electric vector, along two orthogonal directions x and y as [1]:

$$S = \begin{pmatrix} S_0 \\ S_1 \\ S_2 \\ S_3 \end{pmatrix} = \begin{pmatrix} \left\langle E_x E_x^* \right\rangle + \left\langle E_y E_y^* \right\rangle \\ \left\langle E_x E_x^* \right\rangle - \left\langle E_y E_y^* \right\rangle \\ 2\,Re\left(\left\langle E_x E_y^* \right\rangle \right) \\ 2\,Im\left(\left\langle E_x E_y^* \right\rangle \right) \end{pmatrix} \quad (1)$$

It is straightforward to show that

$$S_0^2 \geq S_1^2 + S_2^2 + S_3^2 \quad (2)$$

This condition is known as the physical condition of Stokes formalism. An arbitrary vector that does not satisfy this condition is not a Stokes vector and without any physical meaning.

The general scheme of Stokes images acquisition is illustrated in Figure 1 [1]. The wave reflected from the target, represented by a

Stokes vector S_{in}, is analyzed by a polarization-state analyzer (PSA) by measuring its projections over four linearly independent states. A PSA consists of a linear polarizer (LP) and a quarter wave (QW) rotating about four angles $(\theta_i)_{i=1,4}$. The camera measures the incoming intensities. The complete set of 4 measurements can be written in a vectorial form as:

$$I = AS_{in} \tag{3}$$

I is a 4×1 intensity matrix measured by the camera. The Stokes vector S_{in} can be extracted readily from the raw data matrix I provided that A, the modulation matrix of the PSA, is known by calibration. For the ideal case (theory), matrix A can be given as:

$$A(\theta_i) = \begin{bmatrix} 1 & -cos^2 2\theta_i & -\frac{1}{2}sin\,4\theta_i & sin^2 2\theta_i \\ -1 & cos^2 2\theta_i & \frac{1}{2}sin\,4\theta_i & -sin^2 2\theta_i \\ 0 & 0 & 0 & 0 \\ 0 & 0 & 0 & 0 \end{bmatrix} \tag{4}$$

The angles θ_i are chosen such that the matrix A is invertible. The Stokes image is defined as the measurement of the Stokes vector attached to each pixel.

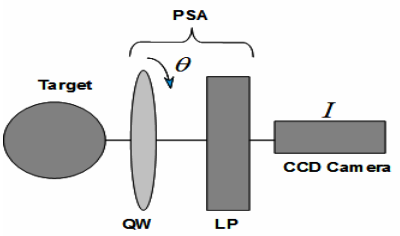

Figure 1 – Stokes imaging device

Figure 2 shows an example of Stokes image acquired in noisy conditions in order to test the performances of the new algorithm. The image is made of 4 small shapes A, B, C, D glued on a cardboard. Objects A and D are transparent.

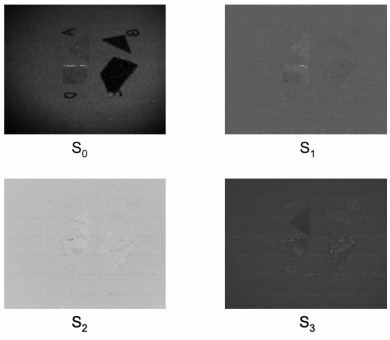

Figure 2 – Stokes image of four small objects glued on a cardboard

2.2 Noise in Stokes images

Noise reaching polarimetric imaging systems lighted with incoherent source light is additive and independent [4]. This type of noise can be modelled by a zero mean random Gaussian distribution which probability density function (PDF) is expressed as follows [6]:

$$f_x(x) = \frac{1}{\sigma_n\sqrt{2\pi}}exp\left(-\frac{x^2}{2\sigma_n^2}\right) \tag{5}$$

Where σ_n^2 is the noise variance. The effect of an additive noise n_a on a digital image g at the pixel position (i,j) is expressed as the sum of the noise free image I and the noise in the form

$$g = I + n_a \tag{6}$$

In perfect acquisition conditions, the Stokes vector is computed on each pixel from equation (3) by

$$S(i,j) = A^{-1}I(i,j) \tag{7}$$

In the presence of noise, this formula becomes:

$$\begin{aligned} \hat{S}(i,j) &= A^{-1}\left(I(i,j) + n_a(i,j)\right) \\ &= A^{-1}I(i,j) + A^{-1}n_a(i,j) \\ &= S(i,j) + \delta S(i,j) \end{aligned} \tag{8}$$

The estimated Stokes vector $\hat{S}$ is an independent sum of the theoritical Stokes vector S and the term δS, due to the additive noise effects. The estimation of the noise distribution is then needed to reconstruct the noisy image δS and eliminate it from the estimated Stokes image $\hat{S}$. However, direct filtering can induce a non physical meaning of the filtered Stokes image $\hat{S} - \delta S$. This means that for an important number of pixels, the vector $\hat{S} - \delta S$ does not satisfy the condition stated in equation (2) and therefeore cannot be considered as a Stokes vector. Without this condition Stokes images don't have any interest for us. For these reasons additional steps will be taken to obtain a tradeoff between filtering and physical meaning for as many pixels as possible.

3. PARAMETRIC NOISE ESTIMATION

Inasmuch as the estimated noised Stokes image is an independent sum of the noise and the noise free image, the estimation of the δS distribution is sufficient to have information about the additive noise. In the context of the multi-dimensionality of Stokes images, we are interested in this work to two multi-spectral filtering methods: Scatter plot method (SP) [6] and data masking method (DM) [4]. The proposed filtering algorithm takes advantages of both methods.
In order to eliminate the impact of the aberrant points, the image is transformed to a Peano-Hilbert fractal path. The new method is tested on gray level images and the results are compared to SP and DM methods. This method is then applied to filter polarimetric images.

3.1 Fractal vectorization filtering algorithm (FVFA)

SP method [6] is not appropriate when dealing with rich textured images. Moreover, this method is time effective because of the calculation of local statistics within the image. DM method [4] is based on the estimation of noise parameters on the residual image given by the convolution of the noisy image with a Laplacian

kernel. Because of the remaining contours, the residual image also contains useful information leading to an overestimation of the noise parameters.
In order to estimate the final noise parameters, our algorithm keeps the idea of calculating the residual image and the use of the local statistics. The remaining limitations of these combined ideas will be compensated by a vectorization of the residual image by the Peano-Hilbert fractal path.
The measured Stokes image is initially filtered by a Laplacian filter in order to suppress the majority of the original image structure and left only the noise attached information. The Laplacian kernel has the following form

$$L = \begin{pmatrix} 1 & -2 & 1 \\ -2 & 4 & -2 \\ 1 & -2 & 1 \end{pmatrix} \tag{9}$$

The remaining edges are detected by applying a Sobel edge detector [8] to the Laplacian convoluted image. A fixed threshold suppresses the pixels considered as belonging to the remaining edges [4]. The residual no-edge image is named the Laplacian image. The Laplacian image is transformed on a vector following a fractal path as presented in a 9×9 image example of Figure 3. The path deals with the Peano-Hilbert fractal path and the vector is designed in the same way as the numbering of Figure 3, from 1 to 81.

1	6	7	48	49	54	55	60	61
2	5	8	47	50	53	56	59	62
3	4	9	46	51	52	57	58	63
16	15	10	45	40	39	70	69	64
17	14	11	44	41	38	71	68	65
18	13	12	43	42	37	72	67	66
19	24	25	30	31	36	73	78	79
20	23	26	29	32	35	74	77	80
21	22	27	28	33	34	75	76	81

Figure 3 – Peano-Hilbert fractal path

Local means μ and standard deviations σ are calculated on the resulted vector by using a shifting interval. The local mean and non-biased standard deviation are respectively defined as:

$$\mu_v(i) = \frac{1}{2m+1}\sum_{k=-m}^{m} v(i+k)$$
$$\sigma_v(i) = \left(\frac{1}{2m}\sum_{k=-m}^{m}\left(v(i+k)-\mu_v(i)\right)^2\right)^{1/2} \tag{10}$$

where v is the portion of the Laplacian image vector limited by the shifting interval of size $2m+1$. These local statistics are the vectorial version of those calculated in SP algorithm applied on the residual no-edges image.
The plane (μ,σ) is then plotted. Two types of points are formed in that plane [6]. The first type is a dense cloud and the second is an isolated set of points corresponding to the remaining edges pixels that are not eliminated by the Sobel filtering. The intersection of linear regression of the cloud points and the y axis gives the better estimation of the noise standard deviation. Similarly, the mean of the noise may be estimated by applying the same instructions on the plotted plane (σ,μ).

The advantage of the fractal path is double: it eases the task of calculating the local statistics within the image with keeping at most the neighbourhood of image pixels. Moreover, the vectorization of the image disperses so much the isolated points of the plane (μ,σ) preventing the regression process from taking them into account. This fact decreases the overestimation of the noise as in the DM method.

3.2 Application to gray level images

To prove the efficiency of the proposed algorithm, three experiments were tested on two gray level images (Figure 4). The first image is a textured checkboard image and the second image is a section of the 3D MRI (Magnetic Resonance Imaging) of the head. The images are both of 256×256 pixels. Additive noises of zero mean with variances 5, 10, 30 and 60 are added to these two images. The noise variance is then estimated by three methods: SP method, DM method, and the proposed algorithm (FVFA). In order to have statistically correct results, the estimated standard deviation $\hat{\sigma}$ is the empirical average of 200 estimations found by the re-sampling Bootstrap method [7]. The dispersion σ_d is then estimated showing that the exact value of the standard deviation lies in the interval $[\hat{\sigma}-3\sigma_d,\hat{\sigma}+3\sigma_d]$ with a probability of 99,73%.

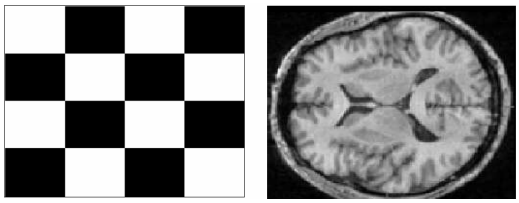

(a) (b)

Figure 4 – Gray level images used to the validation of the proposed algorithm, (a) checkboard, (b) section of a 3D MRI of the head.

The result of the estimation is summarized in Table 1 for the Figure 4. (a) and in Table 2 for the Figure 4. (b). The dispersion σ_d is noted between brackets.

Simulated noise	SP method	DM method	FV method
σ^2	$\hat{\sigma}^2$	$\hat{\sigma}^2$	$\hat{\sigma}^2$
5	10.23[0.5]	9.3[0.41]	5.8[0.04]
10	16.84[0.45]	11.45[0.32]	10.97[0.02]
30	35.09[0.3]	32.75[0.27]	29.59[0.01]
60	63.75[0.27]	62.04[0.12]	60.75[0.01]

Table 1 – Comparison of the noise estimation parameters using SP, DM and FVFA methods on the image of Figure 4. (a).

Simulated noise	SP method	DM method	FV method
σ^2	$\hat{\sigma}^2$	$\hat{\sigma}^2$	$\hat{\sigma}^2$
5	9.13[0.48]	7.8[0.41]	5.4[0.01]
10	13.12[0.41]	11.23[0.3]	9.38[0.01]
30	32.45[0.29]	31.01[0.15]	30.25[0.009]
60	57.41[0.16]	61.08[0.2]	60.09[0.007]

Table 2 – Comparison of the noise estimation parameters using SP, DM and FVFA methods on the image of Figure 4. (b).

The performances of the new method are well visible especially for the textured case of Figure 4. (a). Combined with some physical

considerations in the next section, this method will be chosen to estimate the noise present in polarimetric images.

4. POLARIMETRIC IMAGES FILTERING

4.1 Polarization-based filtering

As seen in section 2 the measured Stokes vector $\hat{S}$ attached to the pixel (i,j) is given as an independent sum of the perfect Stokes vector S_p and an attached noise term $\delta\mathbb{S}$ by:

$$\hat{S}(i,j) = S_p(i,j) + \delta\mathbb{S}(i,j) \tag{11}$$

The term $\delta\mathbb{S}$ is equal to $A^{-1}\delta I$ ($\delta I = n_a$). Under Gaussian assumption of the additive noise, noise parameters are estimated by FVFA method. The intensity noise δI is reconstructed and the polarimetric noise $\delta\mathbb{S}$ is then calculated.

Naturally, the real Stokes vector S_p can be derived from equation (11) by:

$$S_p(i,j) = \hat{S}(i,j) - \delta\mathbb{S}(i,j) \tag{12}$$

Furthermore, the richness information of our images is extremely conditioned by the physical content, .i.e. the vector S_p must satisfy equation 2. However, the direct application of equation (12) to filter polarimetric image induces the non physical behaviour of a large amount of image pixels.

In order to handle this fundamental limitation, a new tool is needed to find the best tradeoff between the filtering and the physical constraint of Stokes images.

The Stokes vector S_p must satisfy equation 2, which is equivalent to the following formula:

$$S_p^T G S_p \geq 0, \qquad G = diag(1,-1,-1,-1) \tag{13}$$

Where $diag$ refers to the diagonal. To control the physical condition on the vector S_p, a parameter α within $[0,1]$ interval is inserted into equation (12) such that:

$$S_p = \hat{S} - \alpha\delta\mathbb{S} \tag{14}$$

If this parameter is too large the physical condition will not be respected whereas if it is too small the filtering is not efficient. The parameter α cannot take negative values; it will result in noise amplification.

Combining equations (13) and (14), one has to search the parameter α that satisfies:

$$\left(\hat{S} - \alpha\delta\mathbb{S}\right)^T G\left(\hat{S} - \alpha\delta\mathbb{S}\right) \geq 0 \tag{15}$$

Developing equation (15), one has to search the parameter α that respects the inequality:

$$\begin{aligned} &f(\alpha) = \left(\hat{S} - \alpha\delta\mathbb{S}\right)^T G\left(\hat{S} - \alpha\delta\mathbb{S}\right) = \\ &\hat{S}^T G\hat{S} - \left(\delta\mathbb{S}^T G\hat{S} - \hat{S}^T G\delta\mathbb{S}\right)\alpha + \left(\delta\mathbb{S}^T G\delta\mathbb{S}\right)\alpha^2 \geq 0 \end{aligned} \tag{16}$$

Assuming that $a = \delta\mathbb{S}^T G\delta\mathbb{S}$, $b = \delta\mathbb{S}^T G\hat{S} - \hat{S}^T G\delta\mathbb{S}$, $c = \hat{S}^T G\hat{S}$ equation (16) is written in the simplified form as:

$$f(\alpha) = a\alpha^2 + b\alpha + c \geq 0 \tag{17}$$

Two real solutions are given by:

$$\alpha = \frac{-b - \sqrt{\Delta}}{2a}, \quad or \quad \alpha = \frac{-b + \sqrt{\Delta}}{2a}, \text{ with } \Delta = b^2 - 4ac$$

Assume that α_1 always refers to the smallest solution and α_2 to the greatest one. For an infinitesimal ε such that if α_i is positive, $\alpha_i - \varepsilon$ is still positive and after the classical resolution of the inequality (17), three cases arise depending on the sign of a:

- $sign(a) > 0$

  If $1 \in [\alpha_1, \alpha_2]$ thus $\alpha = 1$

  If $1 \in [\alpha_1, \alpha_2]$ and $\alpha_1 > 0$ thus $\alpha = \alpha_1 - \varepsilon$

  Otherwise there is no α between 0 and 1

- $sign(a) < 0$

  If $1 \in [-\infty, \alpha_1] \cup [\alpha_2, +\infty]$ thus $\alpha = 1$

  If $0 < \alpha_2 < 1$ thus $\alpha = \alpha_2 - \varepsilon$

  Otherwise there is no α between 0 and 1

- $a = 0$

  One solution exists $\alpha_1 = \alpha_2 = \frac{c}{b}$

  If $0 < \alpha_1 < 1$ thus $\alpha = \alpha_1 - \varepsilon$

  If $\alpha_1 > 1$ thus $\alpha = 1$

  Otherwise there is no α between 0 and 1

These three cases take in account the fact that α must belong to [0,1]

Finally the algorithm can be summarized as:

1. Construct the noise term $\delta\mathbb{S}$ attached to each image pixel by the FVFA method
2. Compute equation (10) for each pixel
3. If the pixel's Stokes vector is physically realisable, set α to 1
4. Otherwise, search the parameter α by following the above instructions.
5. If the discriminate Δ is negative or if there is no α in [0,1], choose the Stokes vector satisfying the maximum between $\hat{S}^T G\hat{S}$ and $S_p^T G S_p$

4.2 Illustration and discussion

Our algorithm is run on two images: simulated Stokes image and a real Stokes image. The synthetic image is built as follows: the Stokes vector at the image center is fixed to $S = \begin{bmatrix} 1 & 1/\sqrt{3} & 1/\sqrt{3} & 1/\sqrt{3} \end{bmatrix}$ (white circular part) and to zero otherwise. Stokes images are multiplied by the modulation matrix A as in equation (3) in order to have the correspondent intensity channels. Relating to the intensity values of the image, a Gaussian noise of zero mean and variance 0.2 is added to the intensity channels. Noisy images are inverted as in equation (7) to get the noisy Stokes image (Figure 5).

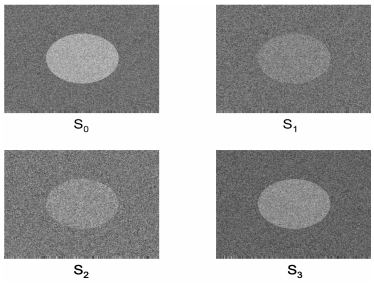

Figure 5 – Noisy Stokes channels. Gaussian zero-mean noise and of variance 0.2 is added to the correspondent intensity channels

The estimated variances using FVFA filtering algorithm on the four intensity channels corresponding to S_0, S_1, S_2 and S_3 are respectively 0.18, 0.19, 0.194 and 0.187. These values are very close to the simulated variance. The results also show that the noise affecting the four polarimetric measurements is roughly the same. The regularization parameter α is calculated for each pixel. Figure 6 shows the binary values of this parameter. Pixels for which α is found between 0 and 1 are set in white otherwise they appear as black pixels.

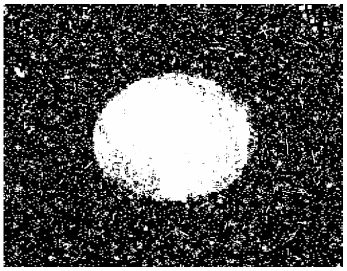

Figure 6 – Binary values of the regularization parameter α

The use of the regularization parameter allows the processing of an important amount of pixels in the image. Indeed without this parameter (equation 12), the image is well filtered but only 10% of the pixels in S_p have physical meaning whereas 70% percent of pixels with the use of parameter α (equation 14). The amount of remaining pixels having no physical meaning is not important. It is due to the fact that conditions 1 to 4 of the algorithm are not satisfied and neither $\hat{S}^T G \hat{S}$ nor $S_p^T G S_p$ are positive (step 5). The result of the two filtering is illustrated in Figure 7. Apparently, the fully filtered image is better, but physically the regularization parameter is preferable and the filtering in this case still acceptable.

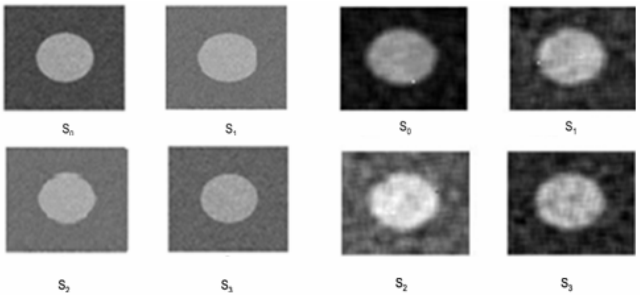

(a) (b)

Figure 7 – Filtered Stokes images with: (a) regularization parameter (equation 10), (b) without regularization parameter (equation 12)

As shown in Figure 7. (a), our algorithm ensures an improvement in polarimetric information carried by Stokes image preserving its physical constraint for most of the pixels.

The real measurement case deals with the Stokes image of Figure 2. As seen in this image, a lot of information are lost, especially in channels S_1, S_2, S_3. Indeed the polarimetric information lies in the three last channels. The inherent noise variances estimated on the correspondent intensity images are respectively up to 10.75, 10.52, 9.78 and 9.88. These values are important compared to the simulated images. This is due to the fact that the intensities are between 0 and 255 for the real image and between 0 and 1 for the simulated image. Results of the physical filtering on noisy Stokes images are presented in Figure 8. The new filtering ensures 64% of physical pixels whereas the classical filtering ensures only 7% of physical pixels. The proposed algorithm is thus a tradeoff between a fully filtered image and a physical constrained (of the most pixels) image.

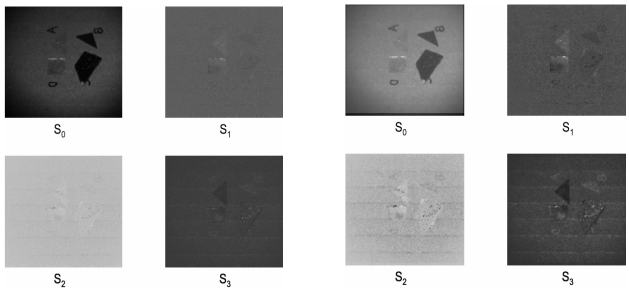

(a) (b)

Figure 8 – (a) Noisy Stokes image, (b) Filtered Stokes image

5. CONCLUSION

A new algorithm to filter polarimetric images is introduced. Based on the filtering methods of multispectral images and combined with a fractal vectorization of the image, the new algorithm is a tradeoff between a classical filtering (noise smoothing) and preserving the physcial meaning of the data. No comparison with other methods is done in this paper, because in the best of our knowledge, this work is the first dealing with the tradeoff between filtering of polarimetric images and preserving the physical condition. Promising results were presented with our method. Multiplicative noise is currently being investigated.

REFERENCES

[1] R.A. Chipman, *"Polarimetry"*, in Handbook of Optics, M. Bass, ed (McGraw-Hill, New York), pp. 22.1-22.36, 1993.

[2] J. Zallat, P. Graebling, and Y.Takakura, "Using polarimetric images for material classification," in *ICIP'03*, Spain,, 2003.

[3] A. Bénière, F. Goudail, M. Alouini and D. Dolfi, "Precision of degree of polarization estimation in the presence of additive Gaussian detector noise," *Optics Communication*, vol. 278, pp. 264–269, Oct. 2007.

[4] A. B. Corner, R. M. Narayanan, and S. E. Reichenbach, "Noise estimation in remote sensing imagery using data masking," in *Int. J. Remote sensing*, vol.4, 2003, pp. 689–702.

[5] J. Zallat, S. Ainouz, and M-P. Stoll "Optimal configuration for imaging polarimeters : impact of image noise and systematic errors ," in *J. Opt.* vol.8, 2006, pp. 807–814.

[6] B. Aiazzi, L. Alparone, A. Barducci, S. Baronti and I. Pippi, "Estimating noise and information of multispectral imagery ," in *Opt. Eng*, vol.41, 2002, pp. 656–668.

[7] R. C. H. Cheng, "Bootstrap methods in computer simulation experiments," in *Simulation Conference Proc.* vol.2, 1995, pp. 171–177.

[8] N. Kazakova, M. Margala, and N. G. Durdle, "Sobel edge detection processor for a real-time volume rendering system," in *ISCAS'04*, vol.2, 2004, pp. 913–916.